

Supplementary Information

Zhou et al.

***Clostridioides difficile* specific DNA adenine methyltransferase CamA squeezes and flips adenine out of DNA helix**

Jujun Zhou<sup>1,3</sup>, John R. Horton<sup>1,3</sup>, Robert M. Blumenthal<sup>2</sup>, Xing Zhang<sup>1,\*</sup>, Xiaodong Cheng<sup>1,\*</sup>

<sup>1</sup>Department of Epigenetics and Molecular Carcinogenesis, University of Texas MD Anderson Cancer Center, Houston, TX 77030, USA

<sup>2</sup>Department of Medical Microbiology and Immunology, and Program in Bioinformatics, The University of Toledo College of Medicine and Life Sciences, Toledo, OH 43614, USA

<sup>3</sup>These authors contributed equally: J.Z. and J.R.H.

\* Correspondence: XZhang21@mdanderson.org or XCheng5@mdanderson.org

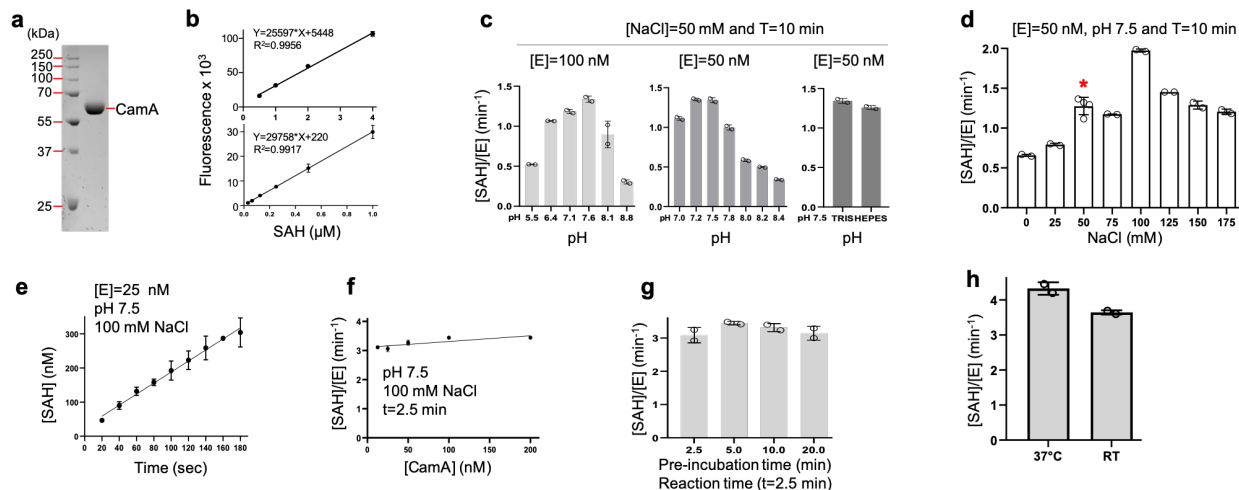
Email addresses:

JZ (JZhou12@mdanderson.org); JRH (JRHorton@mdanderson.org);

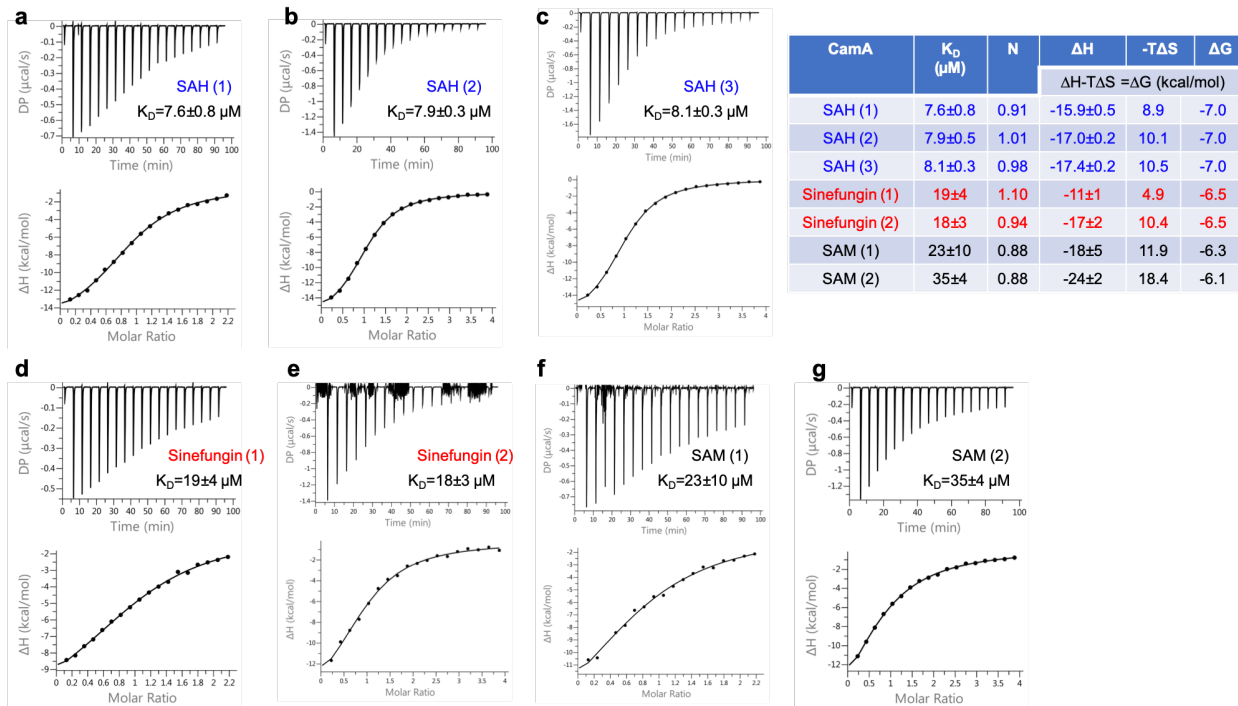
RMB (Robert.Blumenthal@utoledo.edu); XZ (XZhang21@mdanderson.org);

XC (XCheng5@mdanderson.org)

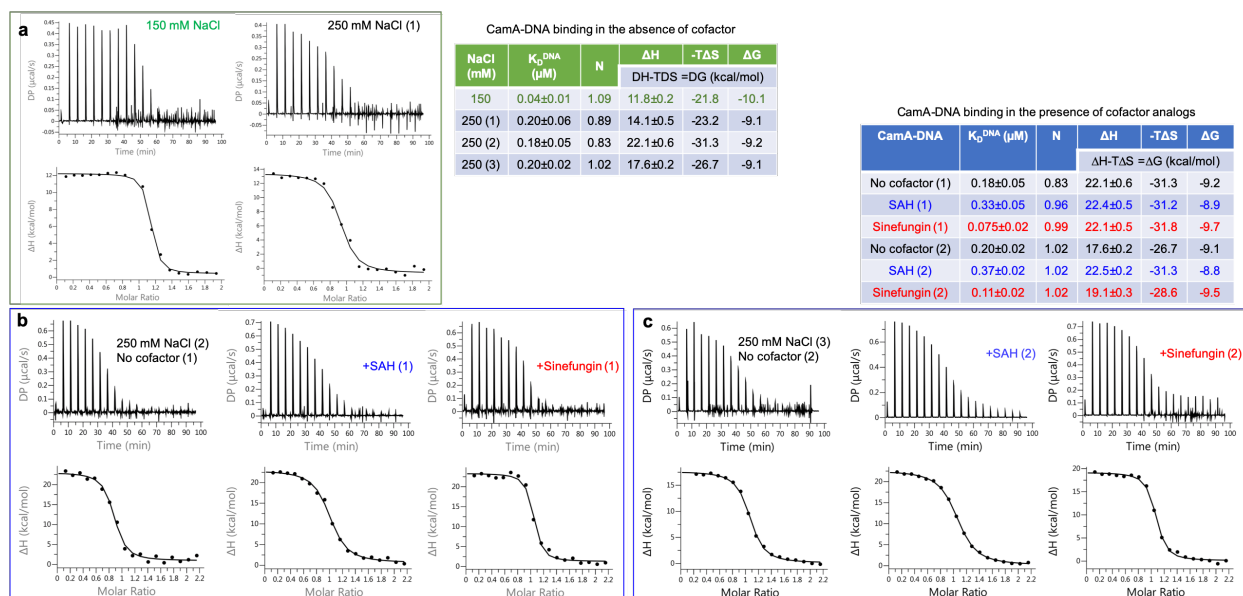
Seven figures and one table



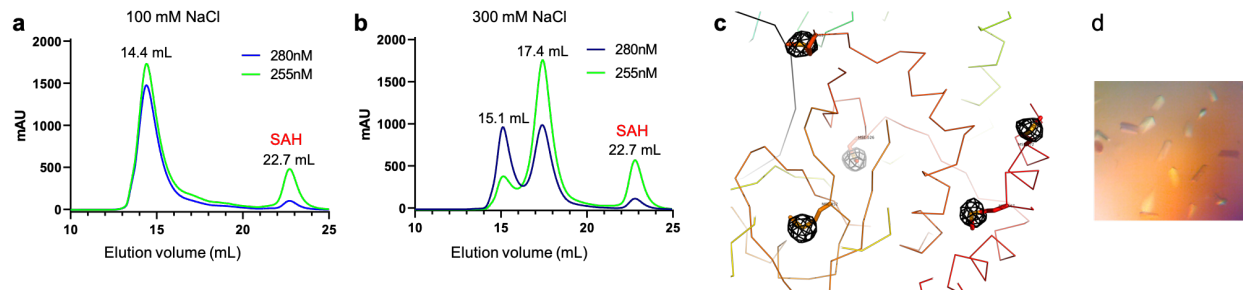
**Supplementary Fig. 1** CamA enzymatic activity. **a** Example of purified recombinant CamA used in the study (12% SDS PAGE with Coomassie blue staining). We purified  $N = 7$  times used for enzyme assays and co-crystallizations. **b** Calibration curves for Promega bioluminescence assay as a function of SAH concentrations in the range of above or below  $1 \mu\text{M}$  (top and bottom panels) ( $N = 2$ ). **c** pH variation ( $N = 2$ ). **d** NaCl variation ( $N = 2$  or 4 as indicated by \*). **e** Reaction time variation ( $N = 2$ ). **f** Enzyme concentration variation ( $N = 2$ ). **g** Variation of pre-incubation time at room temperature ( $N = 2$ ). **h** Comparison of CamA activity on DNA oligo at  $37^\circ\text{C}$  and room temperature (RT;  $\sim 22^\circ\text{C}$ ) ( $N = 2$ ). For convenience, we used room temperature in this study even though CamA has a slightly higher activity at  $37^\circ\text{C}$ . Source data are provided as a Source Data file.



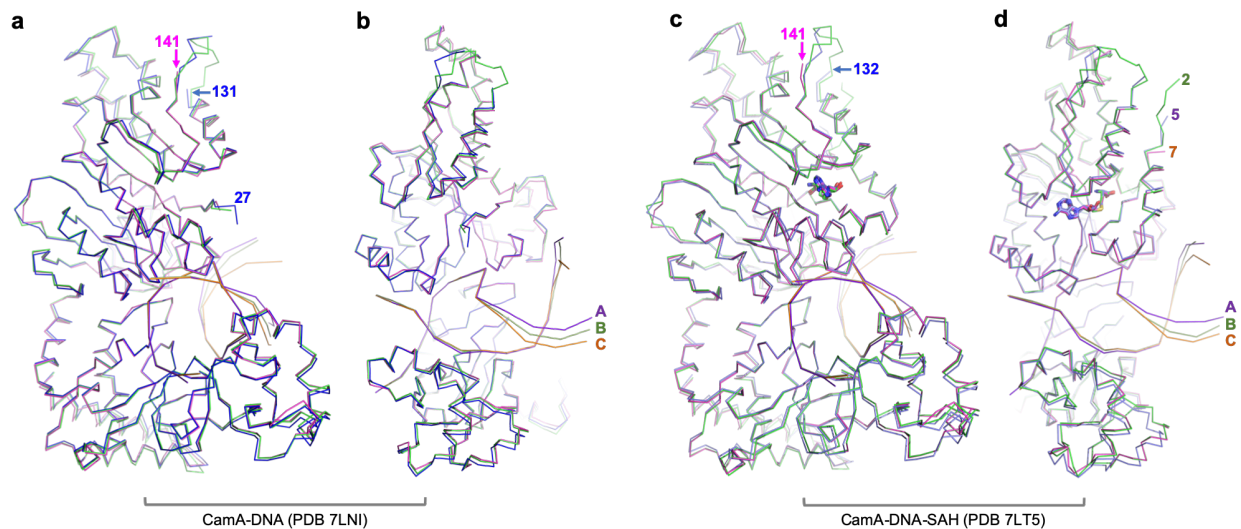
**Supplementary Fig 2.** Isothermal Titration Calorimetry measurements of binding affinity between CamA and cofactor. **a-c** SAH ( $N = 3$ ) with  $[E]=40 \mu\text{M}$  and  $[\text{SAH}]=450 \mu\text{M}$  (**a**) or  $[E]=45 \mu\text{M}$  and  $[\text{SAH}]=900 \mu\text{M}$  (**b-c**). (**D-E**) Sinefungin ( $N = 2$ ) with  $[E]=40 \mu\text{M}$  and  $[\text{sinefungin}]=450 \mu\text{M}$  (**d**) or  $[E]=45 \mu\text{M}$  and  $[\text{sinefungin}]=900 \mu\text{M}$  (**e**). **f-g** SAM ( $N = 2$ ) with  $[E]=40 \mu\text{M}$  and  $[\text{SAM}]=450 \mu\text{M}$  (**f**) or  $[E]=45 \mu\text{M}$  and  $[\text{SAM}]=900 \mu\text{M}$  (**g**). For each experiment, top panel shows the raw microcalorimetry data. The microcalorimeter measures all heat released during the binding until the binding reaction has reached equilibrium. Note that in some experiments we have air bubbles in the sample chamber. Bottom panel shows the enthalpy ( $\Delta H$ ) as the amount of heat released per mole of cofactor bound (kcal/mol). Tabular summary of derived binding affinity ( $K_D$ ), stoichiometry ( $N$ ) and enthalpy and entropy of the binding reaction is provided for each fitting.



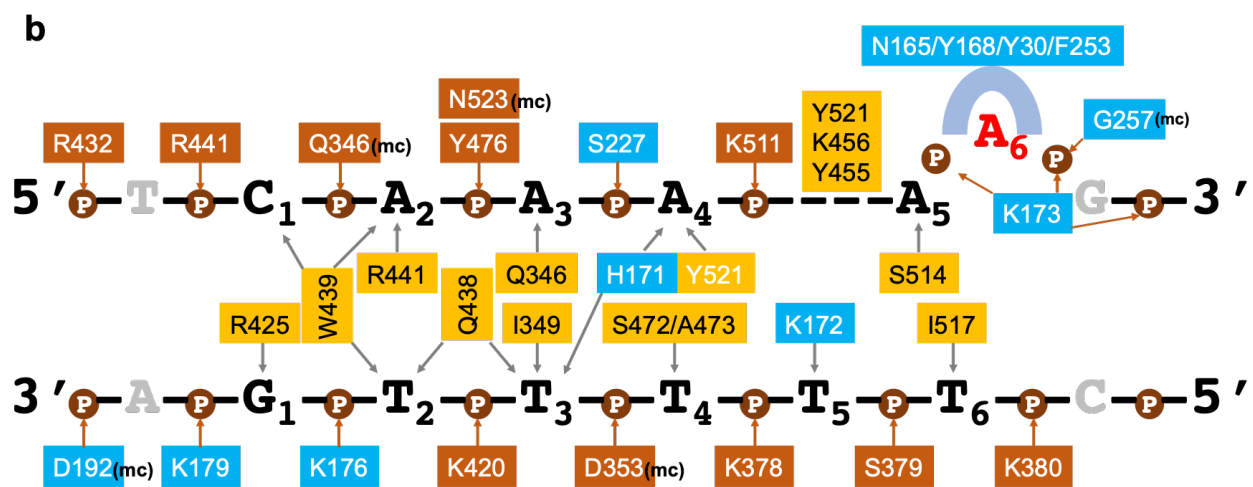
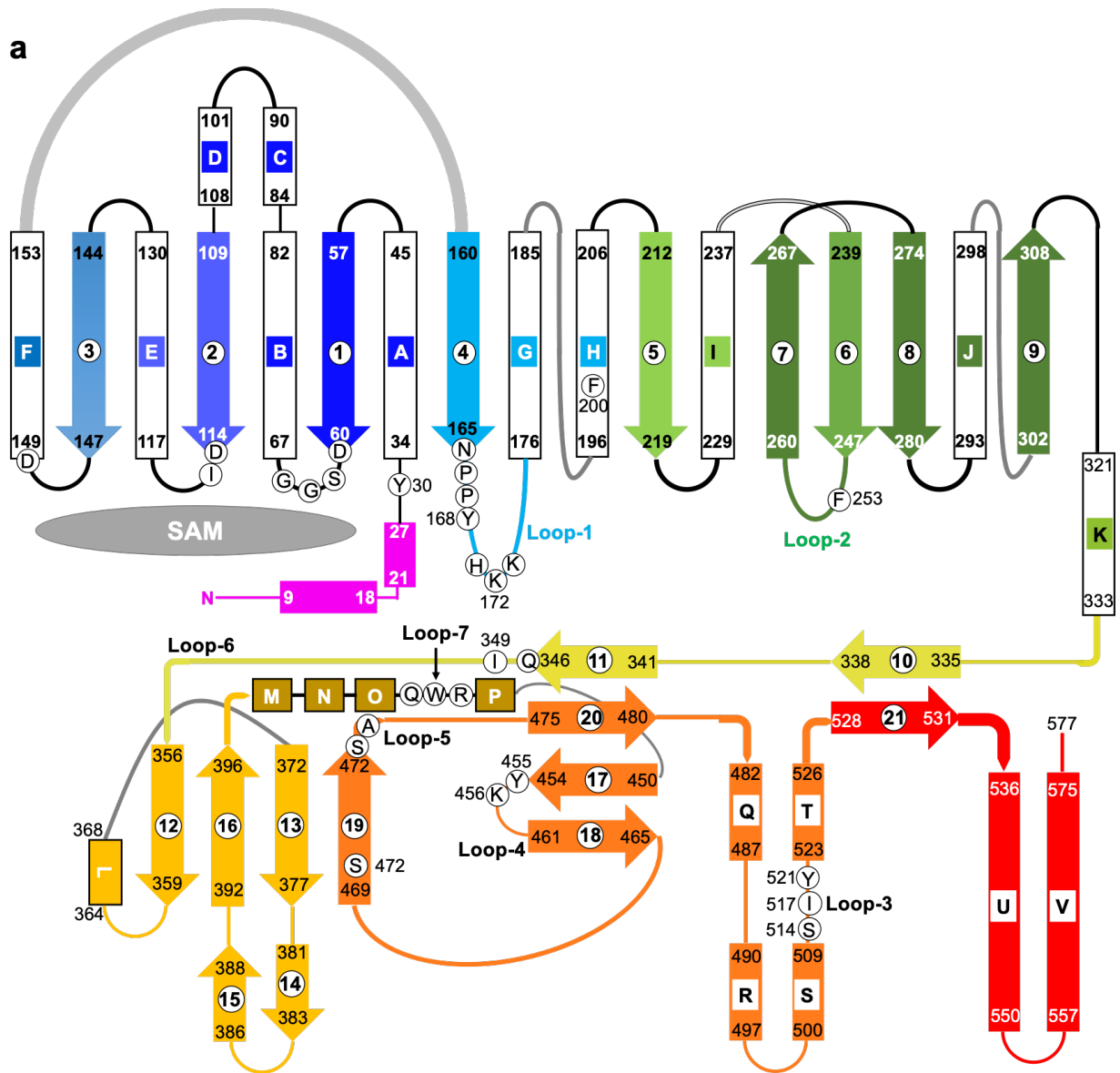
**Supplementary Fig 3.** Isothermal Titration Calorimetry measurements of binding affinity between CamA and DNA. **a** As a function of ionic strength with  $[E]=20 \mu\text{M}$  and  $[DNA]=200 \mu\text{M}$  ( $N = 3$  at 250 mM NaCl). **b-c** In the absence or presence of cofactor analog performed in 250 mM NaCl with  $[E]=18 \mu\text{M}$  and  $[DNA]=200 \mu\text{M}$  ( $N = 2$ ). Tabular summaries of derived binding affinity ( $K_D$ ), stoichiometry ( $N$ ) and entropy and enthalpy of the binding reaction are provided for each fitting.



**Supplementary Fig. 4.** **a-b** Elution profiles of CamA-DNA complexes from sizing exclusion chromatography (Superdex 200 Increase 10/300 GL) under the buffer conditions of 100 mM NaCl (**a**) or 300 mM NaCl (**b**). The protein-DNA complex was stable under 100 mM NaCl, but SAH was dissociated. **c** The anomalous electron density, contoured at  $5\sigma$  above mean, shown for five SeMet residues of the C-terminal TRD domain. **d** Graph of the SeMet-substituted CamA-DNA crystals.



**Supplementary Fig. 5.** Structural comparison of three protein-DNA complexes per asymmetric unit in the space group  $P2_12_12_1$ . **a-b** Two views of protein-DNA complexes in the absence of SAH binding (PDB 7LNI). The largest difference in the protein components lie in the loop region 131-141 away from the protein-DNA interface (**a**), in addition to the disordered N-terminal residues (indicated by residue 27). The largest difference in the bound DNA components is located in the free end of dsDNA lacking any protein contact (**b**). **c-d** Two views of protein-DNA complexes in the presence of SAH (in stick model) (PDB 7LT5).



**Supplementary Fig. 6. a** Schematic diagram of CamA secondary structures, with N-terminal catalytic domain (blue-to-green) and C-terminal TRD (orange-to-red). Helices (rectangles) are labeled from A to V, and strands (arrows) are labeled as 1 to 21. Functional residues, most of them are located in loops L1-to-L7, are labeled with single-letter amino acid abbreviations within white circles. The N-terminal residues undergo conformational changes upon SAH binding are shown in magenta. **b** An enlarged version of schematic of CamA-DNA interactions: residues in cyan background are from the N-terminal catalytic domain, and residues in (light and dark) orange from the C-terminal TRD. The base-specific contacts are placed between the two strands and the phosphate contacts are depicted above or below the strand. mc, main-chain-atom-mediated contacts.



**Supplementary Table 1.** Summary of X-ray data collection and refinement statistics (\*)

CamA	SeMet+DNA	WT+DNA	WT+DNA+SAH
PDB ID	7LNI	7LNJ	7LT5
Wavelength (Å)	0.97795	1.00000	1.00000
Space group	<i>P</i> 2 <sub>1</sub> 2 <sub>1</sub> 2 <sub>1</sub>	<i>P</i> 2 <sub>1</sub> 2 <sub>1</sub> 2 <sub>1</sub>	<i>P</i> 2 <sub>1</sub> 2 <sub>1</sub> 2 <sub>1</sub>
Cell dimensions (Å)	82.07, 160.99, 231.32	82.25, 161.36, 231.63	81.42, 160.86, 230.16
Resolution (Å)	40.76-2.69 (2.79-2.68)	44.35-2.69 (2.79-2.68)	45.10-2.54 (2.64-2.54)
<sup>a</sup> R <sub>merge</sub>	0.308 (0.902)	0.224 (0.940)	0.179 (0.948)
R <sub>pim</sub>	0.053 (0.515)	0.068 (0.690)	0.058 (0.478)
CC <sub>1/2</sub>	(0.671)	(0.384)	(0.564)
<sup>b</sup> <I/σI>	16.1 (1.7)	16.3 (0.9)	10.7 (1.4)
Completeness (%)	99.9 (99.6)	87.8 (73.8)	88.8 (83.1)
Redundancy	32.9 (23.8)	10.3 (7.0)	9.1 (8.7)
Observed reflections	2,825,594	783,940	802,514
Unique reflections	85,923 (8,447)	76,108 (6,312)	88,557 (8,168)
	(78,411 have both I+ and I-)		
Mean FOM (SAD)	0.238		
R-Factor	0.24		
(density modification)			
<b>Refinement</b>			
Resolution (Å)	2.68	2.68	2.54
No. reflections	164,196	75,973	88,478
	(85,819 non-anomalous)		
<sup>c</sup> R <sub>work</sub> / <sup>d</sup> R <sub>free</sub>	0.203 / 0.223	0.210 / 0.251	0.176/0.212
No. Atoms			
Protein	13,371	13,247	13,908
DNA	1704	1686	1686
Solvent	278	124	371
SAH	-	-	78
B Factors (Å <sup>2</sup> )			
Protein	55.7	63.4	49.5
DNA	60.3	67.3	55.1
Solvent	39.0	45.3	37.8
SAH	-	-	47.8
<b>R.m.s. deviations</b>			
Bond lengths (Å)	0.002	0.002	0.002
Bond angles (°)	0.4	0.4	0.5

\* Values in parenthesis correspond to highest resolution shell;

<sup>a</sup> R<sub>merge</sub>=Σ|I-<I>|/ΣI, where I is the observed intensity and <I> is the averaged intensity from multiple observations;

<sup>b</sup> <I/σI> =averaged ratio of the intensity (I) to the error of the intensity (σI);

<sup>c</sup> R<sub>work</sub>=Σ|Fo-Fc|/Σ|Fo|, where Fo and Fc are the observed and calculated structure factors;

<sup>d</sup> R<sub>free</sub> was calculated using a randomly chosen subset (5%) of the reflections not used in refinement.

**Supplementary Fig. 7.** Sequence alignment of CamA orthologs (see following pages).

Only compared CamA orthologs that were nonidentical to the query, in order to more sensitively detect sequence variation. Substitutions are highlighted in cyan, DNA recognition residues in magenta, and universally-conserved residues (with roles as labeled and described in the text) in yellow. The boundary between the catalytic domain and target recognition domain (TRD) is also indicated.











		530	540	550	560	570	
Query	527	KIRIFRDNNYEEIENLSKQIISILLNKSIDKGV	VEKLEKLIKMDNLI	MSLGI	577		
WP_054274745.1	527	KIRIFRDNNYEEIENLSKQIISILLNKSIDKGV	VEKLEKLIKMDNLI	MSLGI	577		
VIB38147.1	527	KIRIFRDNNYDEIENLSKQIISILLNKSIDKGV	VEKLEKLIKMDNLI	MSLGI	577		
WP_009906092.1	527	KIRIFRDNNYDEIENLSKQIISILLNKSIDKGV	VEKLEKLIKMDNLI	MSLGI	577		
WP_003422891.1	527	KIRIFRDNNYDEIENLSKQIISILLNKSIDKGV	VEKLEKLIKMDNLI	MSLGI	577		
WP_107616100.1	527	KIRIFRDNNYDEIENLSKQIISILLNKSIDKGV	VEKLEKLIKMDNLI	MSLGI	577		
VIF75342.1	527	KIRIFRDNNYDEIENLSKQIISILLNKSIDKGV	VEKLEKLIKMDNLI	MSLGI	577		
WP_107619286.1	527	KIRIFRDNNYDEIENLSKQIISILLNKSIDKGV	VEKLEKLIKMDNLI	MSLGI	577		
WP_133143045.1	527	KIRIFRDNNYDEIENLSKQIISILLNKSIDKGV	VEKLEKLIKMDNLI	MSLGI	577		
EGT2204202.1	527	KIRIFRDNNYDEIENLSKQIISILLNKSIDKGV	VEKLEKLIKMDNLI	MSLGI	577		
WP_131040770.1	527	KIRIFRDNNYDEIENLSKQIISILLNKSIDKGV	VEKLEKLIKMDNLI	MSLGI	577		
WP_021385685.1	527	KIRIFRDNNYEEIEISLSRQIISILLNKSIDKGV	VEKLEKLIKMDNLI	MSLGI	577		
WP_054277349.1	527	KIRIFRDNNYEEIEISLSKEIISILLNNSVDKEK	VERLQIKMDNLI	MNSLGI	577		
WP_167640826.1	527	KIRIFRDNNYEEIEISLSKEIISILLNNSVDKEK	VERLQIKMDNLI	MNSLGI	577		
WP_074178811.1	527	KIRIFRDNNYEEIEISLSKEIISILLNNSVDKEK	VERLQIKMDNLI	MNSLGI	577		
NJI79135.1	527	KIRIFRDNNYEEIEISLSKEIISILLNNSVDKEK	VERLQIKMDNLI	MNSLGI	577		
WP_169469916.1	527	KIRIFRDNNYEEIEISLSKQIISILLNNSIDKGV	EMLQIKMDNLI	MSLGI	577		
WP_054271332.1	527	KIRIFRDNNYEEIEISLSKEIISILLNNSVDKEK	VERLQIKMDNLI	MNSLGI	577		
EGT4516689.1	527	KIRIFRDNNYEEIENLSKQIISILLNKSIDKGV	VEKLEKLIKMDNLI	571			
MBH7490777.1	527	KIRIFRDNNYEEIENLSKQIISILLNKSIDKGV	VEKLEKLIKMDNLI	571			
EGT4155821.1	527	KIRIFRDNNYEEIENLSKQIISILLNKSIDKGV	VEKLEKLIKMDN	569			
MBH7182547.1	527	KIRIFRDNNYEEIENLSKQIISILLNKSIDKGV	VEKLEKLIKMDN	563			
MBF9877285.1	527	KIRIFRDNNYEEIENLSKQIISILLNKSIDKGV	VEKLEKLIKMDN	562			
MBG0179561.1	527	KIRIFRDNNYEEIENLSKQIISILLNKSIDKGV	VEKLEKLIKMDN	561			
MBG0197089.1	527	KIRIFRDNNYEEIENLSKQIISILLNKSIDKGV	VEKLEKLIKMDN	560			
EGT3970705.1	527	KIRIFRDNNYEEIENLSKQIISILLNKSIDKGV	VEKLEKLIKMDN	558			
MBG0131288.1	527	KIRIFRDNNYEEIENLSKQIISILLNKSIDKGV	VEKLEKLIKMDN	557			
EGT4149356.1	527	KIRIFRDNNYEEIENLSKQIISILLNKSIDKGV	VEKLEKLIKMDN	546			
EGT3786504.1	527	KIRIFRDNNYEEIENLSKQIISILLNKSIDKGV	VEKLEKLIKMDN	540			
HAU4954234.1	527	KIRIFRDNNYEEIE	540				
WP_131072671.1	527	KIRIFRD	533				
EGT4119714.1	527	KIRIFR	532				
WP_131036696.1	527	KIRI	530				
EGT5091780.1	527	KI	528				